Available online at www.sciencedirect.com

ScienceDirect

Procedia CIRP 38 (2015) 147 – 152

www.elsevier.com/locate/procedia

The Fourth International Conference on Through-life Engineering Services

Degradation Assessment of Industrial Composites using Thermography

Yifan Zhao[a,*], Jörn Mehnen[a], Wei Xu[b], Mosab Alrashed[b], Stephen Abineri[b], Rajkumar Roy[a]

[a]*EPSRC Centre for Innovative Manufacturing in Through-life Engineering Services, UK*
[b]*School of Aerospace, Transport and Manufacturing, Cranfield University, UK*

* Corresponding author. Tel.: +44(0) 1234750111 Ext 2283; fax: +44(0) 1234758292. *E-mail address:* yifan.zhao@cranfield.ac.uk

Abstract

Thermographic inspection is a relatively new technique for Non-Destructive Testing (NDT) which has been gathering increasing interest due to its relatively low cost hardware and extremely fast data acquisition properties. This technique is especially promising in the area of rapid automated damage detection and quantification. In collaboration with a major industry partner from the aerospace sector advanced thermography-based NDT software for impact damaged composites is introduced. The software is based on correlation analysis of time-temperature profiles in combination with an image enhancement process. The prototype software is aiming to a) better visualise the damages in a relatively easy-to-use way and b) automatically and quantitatively measure the properties of the degradation. Knowing that degradation properties play an important role in the identification of degradation types, tests and results on specimens which were artificially damaged have been performed and analyzed.

Peer-review under responsibility of the Programme Chair of the Fourth International Conference on Through-life Engineering Services.
Keywords: NDT; Correlation Analysis; Image Processing; Damage; Inspection

1. Introduction

Composite materials are found in a wide range of applications including the aerospace industry. In fact large proportions of an aircraft are made from composite materials, which include the fuselage, large sections of the wing and the casing surrounding the engine. They are known for their excellent mechanical properties and performance. Unfortunately composites are known to have poor impact resistance. A strike on the panel or surface may cause barely visible impact damage (BVID) but the internal of the composite can be severely damaged. Impacts from birds, stones, hail and even tools from workmen working on the aircraft can cause damage. It has been reported that around 80% of in service damages to composites is caused by impact strikes [1]. As shown in Fig. 1, after an impact on a composite aircraft structure occurred, the significance of the resulting surface defect may not be appreciated because of the very different relationship in composites between surface defect appearance and degradation in performance of the structure [2, 3]. The laminate structure of composite is expected to absorb low velocity impacts either during assembling or in use [4]. When laminate is subjected to even barely visible impact damage, micro-damage is incurred. Its can have a significant effect on the strength, durability, and stability of the laminates [5]. Furthermore, the secondary damage can be developed in the neighboring supporting piles attributed by the primary mode of damage appearing in laminates [6], which makes the inspection more challenging. Table 1 summarises some commonly seen damage types for composites as well as their damage modes.

Table 1. Commonly seen damage types and modes for composites.

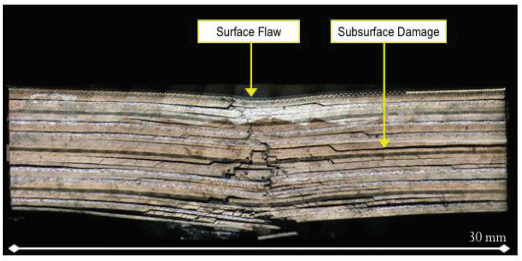

Fig. 1. Cross section through impact damage to a 33 ply, bronze mesh incorporated, painted, CFRP laminate [2].

Peer-review under responsibility of the Programme Chair of the Fourth International Conference on Through-life Engineering Services.
doi:10.1016/j.procir.2015.07.045

Damage Type	Damage Mode
Impact strike	Delamination & Cracking
Heat strike	Deformation & Ablation
Electricity damage	Delamination & Ablation
Creep damage	Delamination & Deformation

The aviation industry has many Non-destructive testing (NDT) methods ranging from basic visual inspection to advanced methods, such as penetrant, magnetic particle, eddy current, radiography, CT, ultrasound and thermography [7]. The range of inspections requires different skills and expertise with varying margins of error. The process of testing the aircraft parts takes place at varying times and is undertaken by pilots, ground crew and even manufactures in some cases. A lot of inspections are simply visually undertaken by ground crew and pilots. However they are not fully versed in detecting anything more than dents with no additional knowledge of the secondary damage, or underlying damage [8]. When further analysis of damage is required a range of advanced techniques are available. Die penetrant testing is a method where penetrant solution is applied to pre-cleaned surface to detect damage. Magnetic particle testing is a method in which defects are detected through using magnetic fields in ferromagnetic components. In eddy current testing, electrical current is passed through a coil to produce a magnetic field, measurement of which is used to detect damage. Radiographic testing uses X-rays for detecting internal damages.

Among the NDT methods, thermography has become a relatively recent addition that has been gathering increasing interests with low cost hardware and fast inspection and data processing. All people and objects emit a certain amount of infrared energy that can be detected and recorded by thermal cameras. They measure heat energy and convert them to electrical impulses, which are displayed as a thermal image with a thermal gradient. There are two classifications of thermography: passive model and active mode. The passive approach tests materials and structures which are naturally at different (often higher) temperature than ambient. Active thermography measures surface temperatures after the application of thermal excitation. This excitation is required to produce a heat signature because usually the parts are in equilibrium with the surrounds. Using this technique, damage and defects can be detected because of the abnormal response to heat transfer, especially for small size components. Thermography has been successfully utilized for several condition monitoring applications such as inspection of civil structures [9], electrical equipment [10], plastic deformations [11], tensile deformation [12], fatigue damages [13], machineries [14] and welding inspection [15]. However, it has not penetrated far into regular use in inspection portfolios for composites components in industry. As far as we are concerned, there are very limited tools available for assessing size of damage area and damage type of composites using thermography inspection. Pointed out by the industry partner, there is a minimum standard of damage size, above which a component can be considered for replacement. Development of such a tool that can identify the size of the damage and tailor to this minimum standard would be a driving factor for this study.

The aim of this study is to develop an image fusion technique that enables a better visualisation and a quantitative and automatic measurement of degradation for industrial composites based on thermographic inspection.

2. Methodology

2.1. Specimens

The specimens were made of unidirectional Toray 800 carbon fibers pre-impregnated with Hexcel M21 epoxy resin. They were cut by water jet cutting into 6 flat plates in the same size of 152.4 ± 0.2mm length, 101.6 ± 0.2mm width and 4 ± 0.2mm thick. One of the specimens is shown in Fig. 2.

Six plates were impacted in the middle with different energy levels using a drop-weight machine. The impactor of this

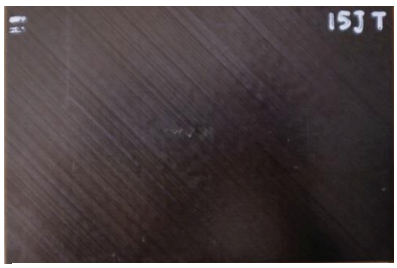

Fig. 2. A standard specimen (impacted side).

machine, as shown in Fig. 3, was semi-spherical, 16mm diameter and 2.281kg weight.

An impact energy was equal to $m \times g \times h$, where m means the mass of impactor, equal to 2.281kg in this experiment; $g = 9.8m/s^2$ means the acceleration due to gravity; h was the drop height. Changing the height of the drop-weight, different energy level could leave different damages in the six specimens. The relationship between drop height and impact energy is shown in Table 2.

Fig. 3. Drop-weight tower.

Table 2. Drop height and impact energy level.

Specimen No.	Drop Height (m)	Energy Level (J)
#1	0.22	5
#2	0.45	10
#3	0.67	15
#4	0.89	20
#5	1.12	25
#6	1.34	30

The six specimens were impacted by 5J, 10J, 15J, 20J, 25J and 30J respectively. The damages could be clearly seen from the impacted side as shown in Fig. 4, but they are invisible or unobvious from the back side, as shown in Fig. 5.

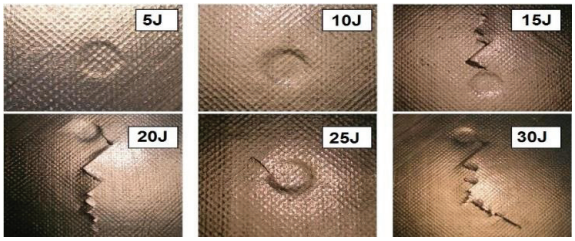

Fig. 4. Visible impact damage from impacted side of the specimens.

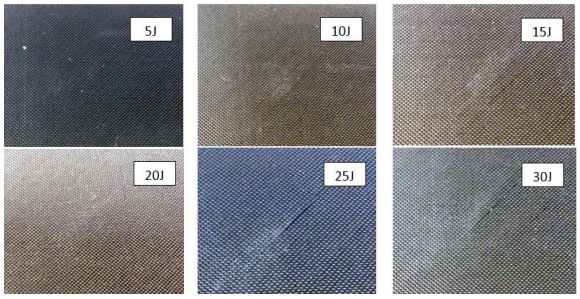

Fig. 5. Invisible or unobvious impact damage from back side of the specimens.

2.2. Experiments

Figure 6 shows the main equipment of the experiments, FLIR SC7000, which is a state-of-the-art infrared technology systems for thermography. The sensor material is InSb or MCT or QWIP, and the filter wheel is motorized, “4 slots for 1” filters, up to 2.5mm thick. The software used to collect data from experiments was *Mosaiq*, by which the thermal images were exported as the form of RAW. The surface of the specimens was positioned to be parallel to the camera lens, and the distance between them was about 30mm. The sampling rate was chosen as 25Hz considering the thickness of the specimens, and 375 frames (duration: 15 sec) were recorded for each testing.

2.3. Proposed image fusion algorithms

Rather than manually choosing a single frame that has the best contrast of damages, this paper proposes an image fusion

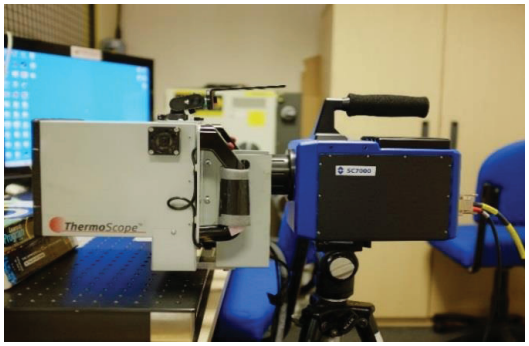

Fig. 6. ThermoScope FLIR SC7000.

technique, which merges a set of images into a single image. This method aims to produce a more informative result with the characteristics of both primary and secondary damages in a single image, which is often impossible for traditional image enhancement techniques for the chosen image.

In the proposed method, the time-temperature profile for each pixel of the thermal image is considered to determine the sound areas and damaged areas. Consider four sampled pixels from the image, two of which were from the sound area and other two were from the damaged area. The log(t) vs log(ΔT) profiles for these four samples are shown in Fig. 7. The value of ΔT was calculated by subtracting the initial temperature before the flash from the current temperature for the considered pixel. Inspection of this figure shows that for sampled pixels from the sound area the temperature cooling curves are close to linear, which is not the case for ones from the damaged area. The new method utilises this characteristics to classify the pixels from sound areas and damaged areas by measuring the similarity between the observed temperature cooling curve and its linear fitting.

The proposed damage visulisation method is summarized as following.

a. Consider a pixel in the thermal image and data of log(t) vs log(ΔT) is collected.

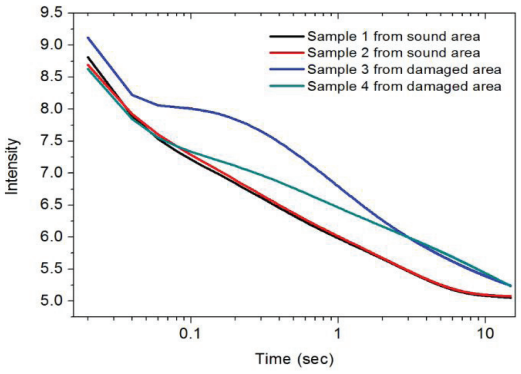

Fig. 7. Time-temperature profiles for 4 selected samples, the first two of which were from the sound area and other two were from the damaged area.

b. Fit the linear curve using least square fitting, where the slope can be assumed known (-0.5) or unknown.
c. Measure the similarity between the fitting and observations through inspection of mean square error (MSE) or correlation coefficient (CC). MSE can be calculated by $MSE = \frac{1}{n}\sum_{i=1}^{n}(\hat{y}_i - y_i)^2$, where $\hat{y}_i$ is the fitting and y_i is the observation, and n is the number of data. The greater value of MSE, the less similarity between observation and the fitting. Correlation coefficient can be calculated by $r = \frac{1}{n-1}\sum_{i=1}^{n}\left(\frac{\hat{y}_i-\bar{\hat{Y}}}{S_{\hat{Y}}}\right)\left(\frac{y_i-\bar{Y}}{S_Y}\right)$, where $\bar{Y}$ and $\bar{\hat{Y}}$ are the means of the fitting and observation respectively; $S_{\hat{Y}}$ and S_Y are the standard deviations of the fitting and observation respectively. The absolute value was considered in this paper, so the result will vary from 0 to 1. The greater value of correlation coefficient, the higher similarity between the fitting and observations.
d. Repeat step a-c for all pixels in the image and produce of a map of MSE or correlation coefficient.
e. Normalise the map to achieve the optimal visualisation.

After above steps for damage visualisation, image processing techniques were used to segment the primary and secondary damages as well as measuring their properties. This process can be summarized as

1) Implement a 5 by 5 mean filter to remove the noise.
2) Enhance the contrast between sound areas and damaged areas using a contrast stretch technique.
3) Extract the primary damage and secondary damage by selecting appropriate thresholds.
4) Implement the image segmentation approach to segment each region of damages.
5) Quantitatively measure the properties of each region (e.g. location, area, perimeter, bounding box).

2.4. Prototype software

A new prototype software was developed, named Infrared Damage Enchantment and Analysis (IDEA), as the implementation of the developed technique. IDEA was developed and ran on MATLAB R2014a which was installed on Windows 7 (64-bit Operating System) in a PC. This software provides the capability to visualise and measure the damages through initially choosing the region of interest (ROI), the number of images to be analysed and then applying the proposed method. Figure 8 shows a snapshot of IDEA control panel, where the left panel controls the display, the middle panel manages the color and selected ROI, and the right panel provides four visualisation algorithms. These four algorithms are correlation coefficient with slope fixed linear fitting (CC-SFF), MSE with slope fixed linear fitting (MSE-SFF), correlation coefficient with slope unknown linear fitting (CC-SUF) and MSE with slope unknown linear fitting (MSE-SUF). The results can be visualised in the form of 2D image with a 'jet' colormap or 3D surface. Measurement tools are also provided to calculate the properties of the detected primary and secondary damages (e.g. location, area, perimeter, bounding box).

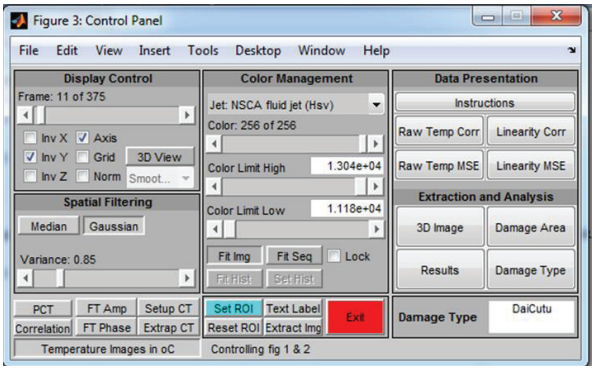

Fig. 8. IDEA Control Panel.

3. Results

3.1. Visualisation

The 15J specimen was tested by capturing the thermal images from the back side and 250 frames were analysed by four proposed visualisation algorithms. Results are shown in Fig. 9, where the bright areas indicate the primary damage and the dark blue 's' shape indicates the secondary damage. CC-SFF and CC-SUF have a similar performance with relatively less noise on the background. MSE-SUF can better visualise the material structure of the sound areas. MSE-SFF has a good contrast for the primary damage but less contrast for the secondary damage. Collectively, results show that all four algorithms have the capability to display the primary and secondary damage in one image. Figure 10 shows an alternative way to visualise the damage in 3D surface. By rotating the 3D view, the damages can be inspected in more details. The volley between two high peaks indicates a possible air gap that occurred during the damaging of the composite. The lowest level refers to the compressed areas that probably

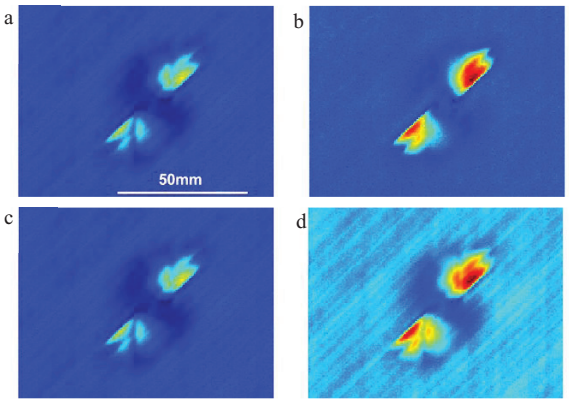

Fig. 9. Produced visualisation of damage, where the 'jet' colormap was used to indicate the similarity between the observed curve of log(temperature) vs log(time) and its linear fitting. (a) CC-SFF. (b) MSE-SFF. (c) CC-SUF. (d) MSE-SUF.

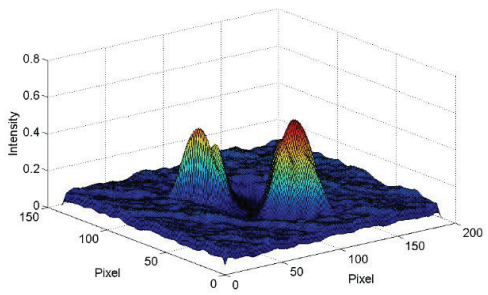

Fig. 10. 3D view for the detected damage for 15J using CC-SFF (1 mm = 2.8 pixels).

because the compression does not conduct any heat during the thermal imaging.

3.2. Measurement

Primary and secondary damages were extracted through two thresholds and the results are shown in Fig. 11. Table 3 shows some measured properties for each segmented region, which include the area, the left top coordinates of the bounding box and the position and dimension (width and height). More

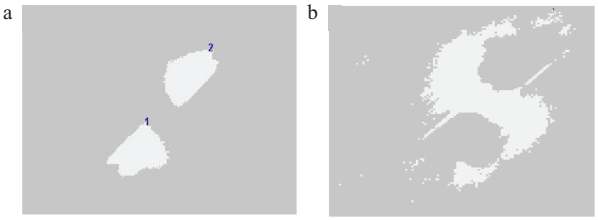

Fig. 11. Extracted (a) primary and (b) secondary damage for 15J using CC-SFF.

morphological properties can be easily calculated, some of which may play an important role to identify the type of damage.

Table 3. Measured properties for each segmented region of 15J.

Region No.	Mode	Area (pixels)	Area (mm^2)	Bounding box [X;Y;W;H] (pixels)
1	Primary	755	92.07	[64.50;72.50; 41; 34]
2	Primary	776	94.63	[101.50;27.50;36;36]
3	Secondary	2211	269.63	[15.5; 3.5; 111; 122]

All six specimens have been analysed by the proposed routine. The visualisation results are shown in Fig. 12 and measured total damage area in mm^2 versus the impact factor is shown in Fig.13 with the same thresholds. Inspection of Fig. 12 shows that the secondary damages were detected for all specimens, while the primary damages were detected for specimens with impact energy no less than 10 joules. For the specimen 5J, the primary damage probably is too weak to be detected by thermal inspection. Figure 13 obviously shows that the higher the impact energy, the larger the delamination area detected.

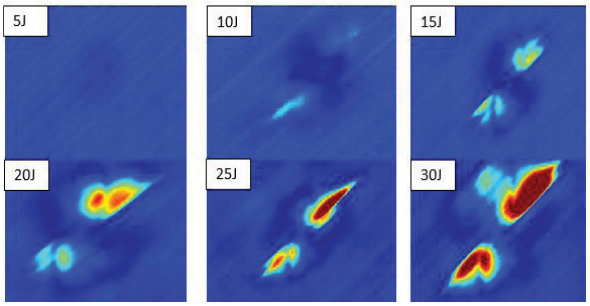

Fig. 12. Produced visualisation of damage for all six specimens using CC-SFF by considering 250 thermal images from the back side of the specimen.

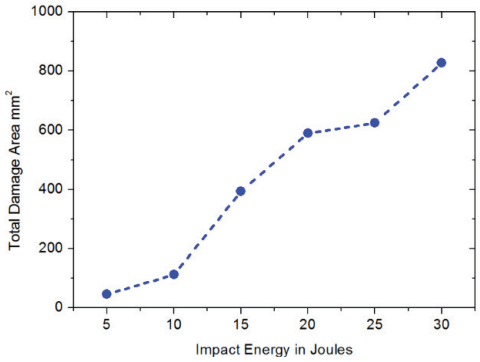

Fig. 13. Measured total areas of damage for all 6 specimens.

4. Conclusions

The degradation assessment of industrial composite materials using thermography was verified practically using thermography and the developed prototype software, Infrared Damage Enhancement and Analysis (IDEA). IDEA was found to be effective and efficient in analysing the subsurface damage in composites by analysing images from pulse thermography testing.

Four algorithms based on the similarity between the observations of time-temperature profile and its linear fitting have been developed. An image noise-removal and enhancement process then followed to achieve the best visualisation of primary and secondary damages in one image. An analysing routine was then introduced at the end to quantitatively measure the properties of each region of damages.

Conventionally, for example, a single image that has the maximum contrast for a primary damage is chosen for visualisation purpose. To visualise the secondary damage, another single image has to be chosen. This study developed an image fusion technique that takes into account a batch of images and then produces one image that has the optimal visualisation for both damages in a single image. This technique simplifies the inspection process in a relatively easy-to-use way, and also facilitates the development of automatic thermal inspection. A 3D view capability was also developed to enable a more intuitionistic inspection way. All capabilities

have been tested and validated by six artificially impacted specimens.

There is still some further work to be undertaken to refine this technique. Firstly, the first and second derivative of time-temperature data as well as thermal signal reconstruction (TSR®) [16] can be integrated into the proposed technique to measure the depth of the delamination. Secondly, more experiments have to be performed for specimens with various materials and damages to characterise their damage profile through thermography, which is the key to develop the capability to identify the type of degradation for composite component.

Acknowledgements

This work was supported by the EPSRC Centre for Innovative Manufacturing in Through-life Engineering Services (Grant number EP/I033246/1) and by a core industrial partner.

References

[1] Civil Aviation Authority Safety Regulation Group, CAP562 Civil Aircraft Airworthiness Information and Procedures, Issue 2, Amendment 1, 2005.
[2] G. Newaz, R. L. Sierakowski (1995). Damage tolerance in advanced composites, CRC Press.
[3] S. Sanchez-Saez, E. Barbero, R. Zaera, C. Navarro (2005). Compression after impact of thin composite laminates. Composites Science and Technology, vol. 65(13), pp. 1911–1919.
[4] T. W. Shyr, Y. H. Pan (2003). Impact resistance and damage characteristics of composite laminates. Composite Structures, vol. 62(2), pp. 193-203.
[5] M. Freitas, L. Reis (1998). Failure mechanisms on composite specimens subjected to compression after impact. Composite Structures, vol. 42, pp. 365–373.
[6] D. T. G. Katerelos, J. Varna (2012). Secondary damage effect on stress redistribution in laminated composites. International Journal of Damage Mechanics. vol. 22(5), pp.752-769.
[7] A. Kapadia (1983). Non-Destructive Testing of Composite Materials. london: TWI. 10-20.
[8] I.G. Scott, C.M. Scala (1982). A review of non-destructive testing of composite materials, NDT International, vol. 15(2), pp. 75-86.
[9] E. Grinzato, C. Bressan, S. Marinetti, P.G. Bison, C. Bonacina (2002). Monitoring of the Scrovegni Chapel by IR thermography: Giotto at infrared, Infrared Physics & Technology, vol. 43, pp. 165–169.
[10] M.S. Jadin, S. Taib (2012). Recent progress in diagnosing the reliability of electrical equipment by using infrared thermography, Infrared Physics & Technology, vol. 55, pp. 236–245.
[11] C. Badulescu, M. Grediac, H. Haddadi, J.-D. Mathias, X. Balandraud, H.-S. Tran (2011). Applying the grid method and infrared thermography to investigate plastic deformation in aluminium multicrystal, Mechanics of Materials, vol. 43, pp. 36–53.
[12] B. Venkataraman, B. Raj, C.K. Mukhopadhyay, T. Jayakumar (2001). Correlation of infrared thermographic patterns and acoustic emission signals with tensile deformation and fracture processes, in: D.O. Thompson, D.E. Chiment (Eds.), Review of Progress in Quantitative Nondestructive, Evaluation, vol. 557, pp. 1443–1450.
[13] M.P. Luong (1998). Fatigue limit evaluation of metals using an infrared thermographic technique, Mechanics of Materials, vol. 28, pp. 155–163.
[14] S. Bagavathiappan, T. Saravanan, N.P. George, J. Philip, T. Jayakumar, B. Raj (2008). Condition monitoring of exhaust system blowers using infrared thermography, Insight, vol. 50, pp. 512–515.
[15] C. Meola, G. M. Carlomagno, A. Squillace, G. Giorleo (2004). The use of infrared thermography for nondestructive evaluation of joints, Infrared Physics & Technology, vol. 46, pp. 93–99.
[16] S. M. Shepard, J. R. Lhota, B. A. Rubadeux, D. Wang, T. Ahmed (2003). Reconstruction and enhancement of active thermographic image sequences, Optical Engineering, vol. 42(5), pp. 1337-1342.

2015-10

Degradation assessment of industrial composites using thermography

Zhao, Yifan

Elsevier

Yifan Zhao, Jörn Mehnen, Wei Xu, Mosab Alrashed, Stephen Abineri, Rajkumar Roy. Degradation assessment of industrial composites using thermography. 4th International Conference on Through-Life Engineering Services, 3-4 November 2015, Cranfield University, Cranfield, UK. Procedia CIRP, Volume 38, 2015, Pages 147-152

http://dx.doi.org/10.1016/j.procir.2015.07.045